Electronic Supplementary Material (ESI) for Chemical Communications.
This journal is © The Royal Society of Chemistry 2018

Supporting Information

The impact of grafted surface defects on the on-surface Schiff-base chemistry at the solid-liquid interface.

Nerea Bilbao,[†a] Yanxia Yu,[†bc] Lander Verstraete,[a] Jianbin Lin,[d] Shengbin Lei,*[bc] and Steven De Feyter *[a]

[a]Department of Chemistry, Division of Molecular Imaging and Photonics, KU Leuven – University of Leuven, Celestijnenlaan 200F, B-3001 Leuven, Belgium.
[b]School of Chemistry and Chemical Engineering, Harbin Institute of Technology, Harbin, 150080, P. R. China.
[c]Tianjin Key Laboratory of Molecular Optoelectronic Science, Department of Chemistry, School of Science & Collaborative Innovation Center of Chemical Science and Engineering (Tianjin), Tianjin University, Tianjin, 300072, P. R. China.
[d]Department of Chemistry, College of Chemistry and Chemical Engineering, and MOE Key Laboratory of Analytical Sciences, Xiamen University, Xiamen 361005, P. R. China.

[†]These authors contributed equally.

TABLE OF CONTENTS

S0. STM experimental details.

All experiments were performed at room temperature (20°C - 22°C) using a PicoLE (Keysight) or Molecular Imaging STM system in constant-current mode. STM tips were prepared by mechanical cutting from Pt/Ir wire (80/20, diameter 0.25 mm, Advent Research Materials). HOPG (grade ZYB, Momentive Performance Material Quartz Inc., Strongsville, OH, USA) was used as substrate for STM measurements at the solid-liquid interface and under ambient conditions. Several samples were investigated, and for each sample, several locations were probed. The bias voltage refers to the substrate. STM images were processed using Scanning Probe Image Processor (SPIP, Image Metrology ApS) and WSxM (NanotecElectronica, Spain)[1] softwares. Nanoshaving of corrals in the covalently modified HOPG was performed using the Keysight PicoLITH 2.1 software. Imaging parameters for the STM images are indicated in the figure captions and denoted by V_{bias} for sample bias and I_{set} for tunneling current.

S1. Covalent modification of HOPG using cyclic voltammetry.

Electrochemical grafting of 3,5-bis-*tert*-butylbenzenediazonium (TBD) was carried out according to previously reported procedures,[2, 3] and performed using cyclic voltammetry in aqueous solutions. Due to its low stability, TBD was generated *in situ* from the corresponding aniline 3,5-bis-*tert*-butylaniline. The electrochemical modification of the HOPG samples was carried out in a lab-built single-compartment three-electrode cell, with a working electrode area of 38.5 mm^2, a Pt wire counter and Ag/AgCl/3M NaCl reference electrodes. 5 mL of 3,5-bis-*tert*-butylaniline (0.1 and 0.4 mM) in 0.05 M HCl aqueous solution was mixed with aqueous $NaNO_2$ (0.1 mL, 0.1 M), and after approximately 90 s the mixture was injected into an electrochemical cell to run cyclic voltammetry (3 cycles, range: 0.6 to -0.35 V, scanning rate: 100 mV s^{-1}). Prior to each experiment, the HOPG working electrode was freshly cleaved using Scotch tape. After modification, the TBD modified HOPG samples were rinsed with Milli-Q water to remove any physisorbed material from the surface. 3,5-bis-*tert*-butylaniline (98%) and analytical grade hydrochloric acid were purchased from Sigma-Aldrich and used without further purification. High-purity water (Milli-Q, Millipore, 18.2 MΩ cm, TOC < 3 ppb) was used for preparation of the aqueous solutions. All electrochemical measurements were performed using an Autolab PGSTAT101 potentiostat (Metrohm_Autolab BV, The Netherlands).

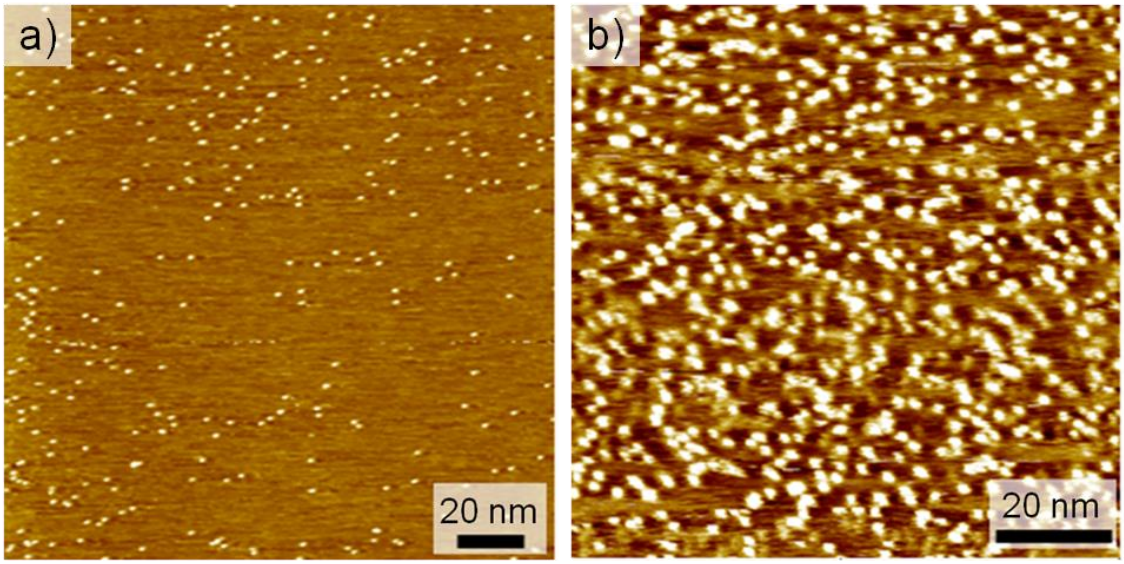

Figure S1. STM images after grafting of TBD on HOPG from (a) 0.1 mM (6000-14000 pins *per* μm^2) and (b) 0.4 mM (60000-90000 pins *per* μm^2) solutions. Imaging conditions: (a) I_{set} = 50 pA, V_{bias} = -0.60 V; (b) I_{set}=70 pA, V_{bias} = -0.60 V.

S2. On-surface synthesis of imine-based single-layer covalent organic frameworks on bare HOPG.

The on-surface synthesis of imine-based sCOFs on bare HOPG was performed according to a previously reported procedure.[4] Owing to the limited solubility of the chemicals in octanoic acid, all building blocks were first dissolved in dimethylsulfoxide (DMSO, >99.0% Sigma-Aldrich), and then, the solution was diluted in octanoic acid (>98.0% TCI) to a designated concentration, indicated in each case. BTA, PDA and DATP were commercially purchased from Sigma-Aldrich and used without further purification. AABA was synthesized following the previously reported methodology.[5] For the on-surface synthesis at the solid-liquid interface at room temperature, the aromatic amine and aromatic aldehyde octanoic acid solutions were mixed in a 2:3 molar ratio, and 5 µL of the mixed solution were drop-casted on the freshly cleaved HOPG surface or covalently-modified HOPG substrate at room temperature. The resulting reaction product was characterized by scanning tunneling microscopy (STM). Figure S2 corresponds to the on-surface synthesis of the three imine-based sCOFs on bare HOPG. Following this reported procedure, extended sCOF networks with very few defects could be achieved for the three systems. Characteristic and previously reported defects for these systems are typically missing linkers, 7- and 5-membered rings,[6-9] and polymer-free areas.[10] On bare HOPG, an average of 10 000–20 000 defects/µm^2 could be accounted for the three sCOF products.

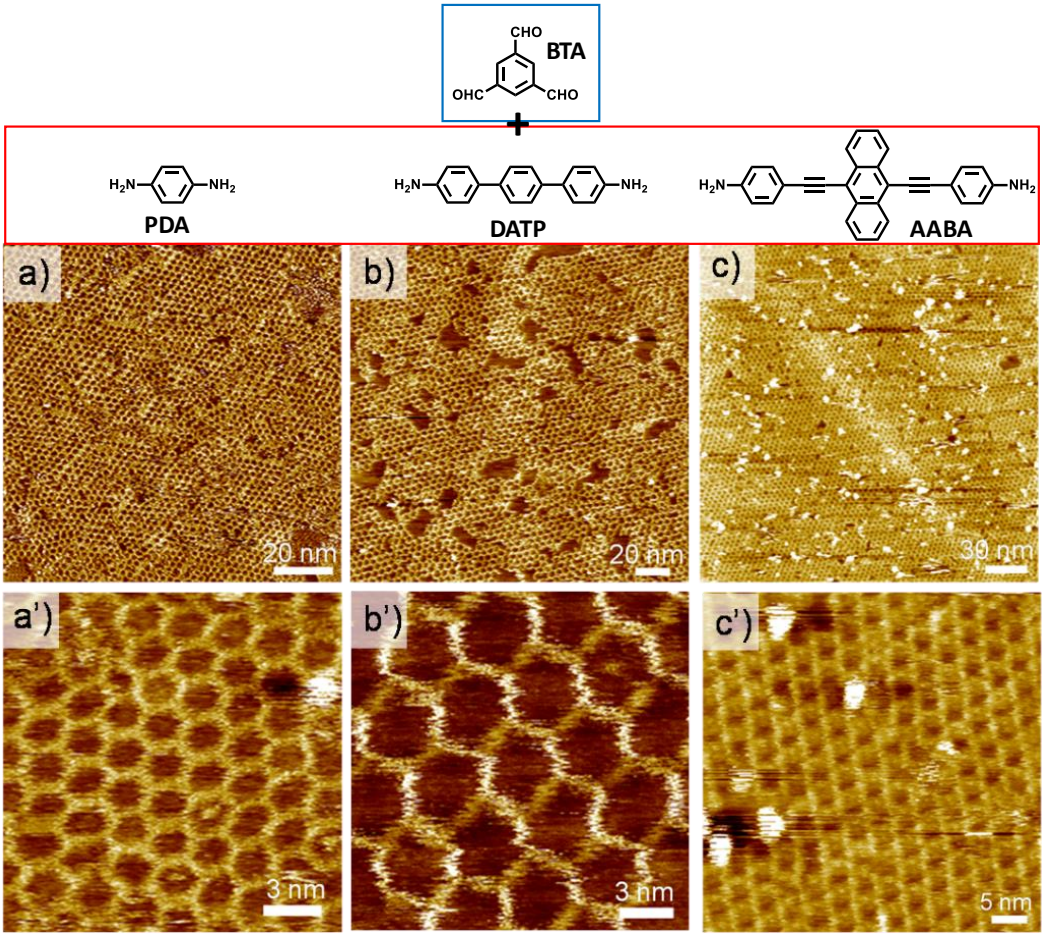

Figure S2. STM images of the 2D sCOFs formed onto bare HOPG at the solid-liquid interface (the di-amine monomer concentration in octanoic acid is given between parenthesis): (a, a') $sCOF_{BTA\text{-}PDA}$ (0.01 mg/g), (b,b') $sCOF_{BTA\text{-}DATP}$ (0.005 mg/g), (c,c') $sCOF_{BTA\text{-}AABA}$ (0.004 mg/g). The occasional white spots observed above the networks are attributed to either unreacted monomers or covalent aggregates. Imaging conditions: (a, a') I_{set} = 60 pA, V_{bias} = -0.66 V; (b,b') I_{set} = 50 pA, V_{bias} = -0.66 V; (c,c') I_{set} = 700 pA, V_{bias} = -0.7 V.

S3. On-surface synthesis of imine-based sCOFs on modified HOPG surfaces with variable density of grafting.

Figure S3a and S3b correspond to large fully covered modified surface (variable density grafting) by the sCOF formed by the BTA and DATP molecules. These images give an indication of the adaptability of the on-surface Schiff base chemistry, as the system perfectly accommodates around the grafted bulky aryl species and affords an almost defect-free 2D porous polymer at room temperature and under ambient conditions.

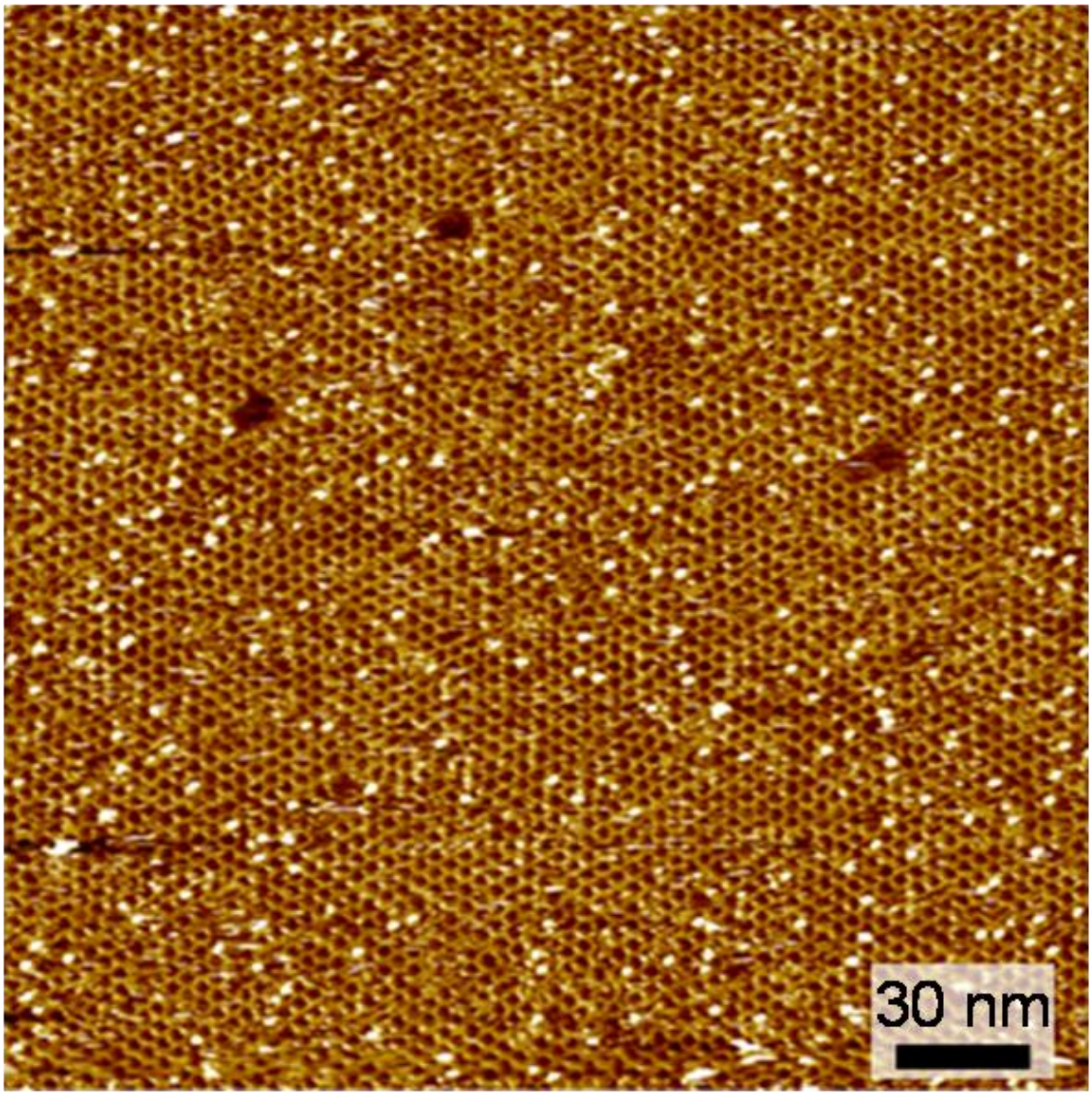

Figure S3a. Large scale STM image (252 x 252 nm^2) of the sCOF formed by BTA and DATP ($sCOF_{BTA\text{-}DATP}$) on modified HOPG with low density of grafted TBD species (6000–14000 pins *per* μm^2). Imaging conditions: I_{set} = 120 pA, V_{bias} = -0.66 V. The domains are medium- to large-sized and cover 98% of the surface. About 25 000–35 000 defects could be accounted per μm^2 (only 5-, 7-membered rings and missing linkers considered).

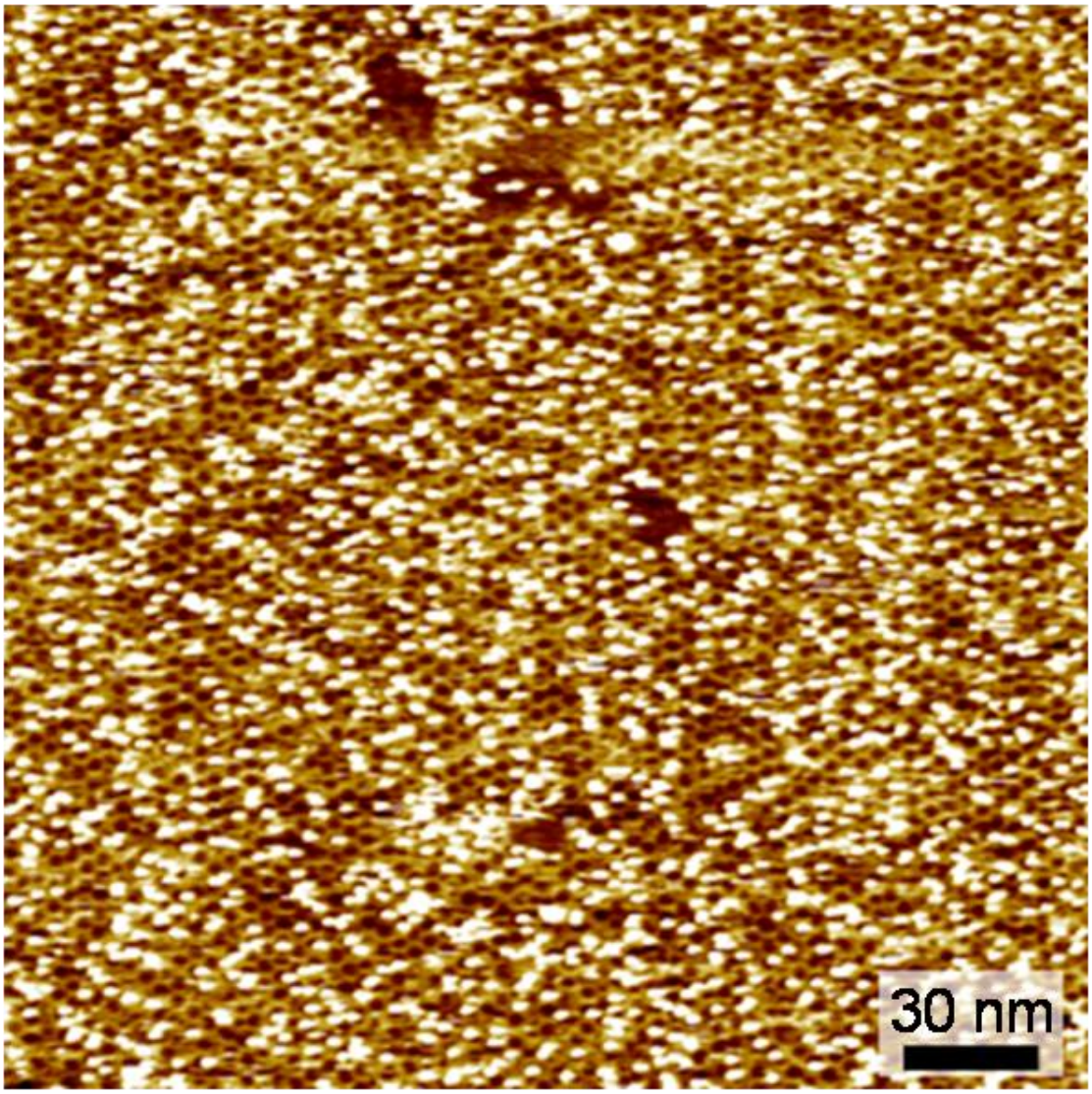

Figure S3b. Large STM image (236 x 236 nm^2) of $sCOF_{BTA\text{-}DATP}$ on modified HOPG with high density of grafted species (60000–90000 pins *per* um^2). Imaging conditions: I_{set} = 50 pA, V_{bias} = -0.66 V. Here, although the surface coverage is maintained as high as 98%, the number of smaller domains has increased greatly. The dispersity of flake sizes is also broader because of the circumstantial local agglomeration or absence of grafted molecules.

Table S3c displays the surface coverage registered for the three studied sCOF systems on low and high density of grafted species (6000–14000 and 60000–90000 pins/µm^2, respectively). When carrying out the reaction on freshly cleaved bare HOPG, an extended network of sCOF could be obtained with a surface coverage > 94% (for the three imine-based systems). This table indicates, as well, the number of defects *per* µm^2 observed on bare HOPG, and when incorporating TBD grafted molecules but keeping the grafting density low. Only missing linkers, 7- or 5-membered rings in the network were considered as defects, and not sCOF-free areas. When the grafting density becomes too high, the size of the domains is too low to accurately count the number of network defects.

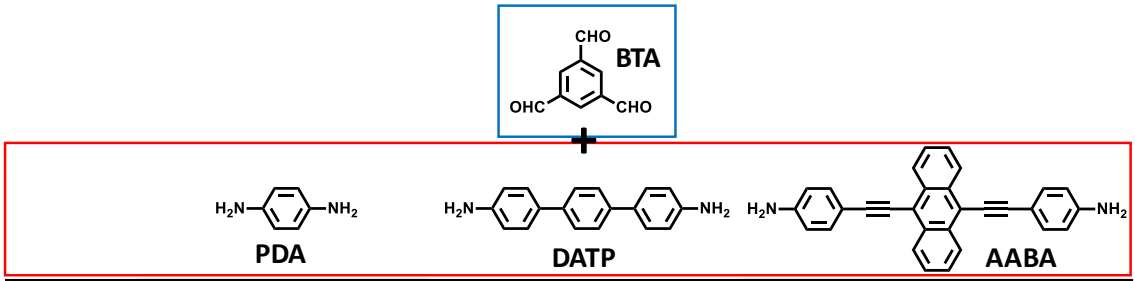

Coverage on low density grafting	88%	98%	82%
Coverage on high density grafting	86%	98%	X
Number of defects *per* µm^2 on bare HOPG	10 000–20 000	10 000–20 000	10 000–20 000
Number of defects *per* µm^2 on low density grafted surfaces	18 000–29 000	25 000–35 000	18 000–22 000

Table S3c. Table summarizing the surface coverage and number of defects *per* µm^2 estimated for the three studied sCOF systems on low and high density of grafted species (6000–14000 and 60000–90000 pins *per* µm^2, respectively).

The size of the domains was typically as large as the scanned area for the three sCOF systems grown on bare HOPG. As grafted TBD molecules are incorporated in the surface, some effects such as the splitting of the edges of the framework, corresponding to the coexistence of two neighboring sCOF flakes, or the presence of a cluster of TBD grafted molecules forming a domain boundary, could be observed in the STM images (see red arrows in Fig. S3d). The larger the surface area of the precursor, but specially the smaller the pore of the sCOF formed, the higher the number of domain boundaries and the smaller the domain size. $sCOF_{BTA\text{-}DATP}$ is the system that adapts better to the restricted space *via* the incorporation of more network defects and consequently covers most of the available HOPG surface.

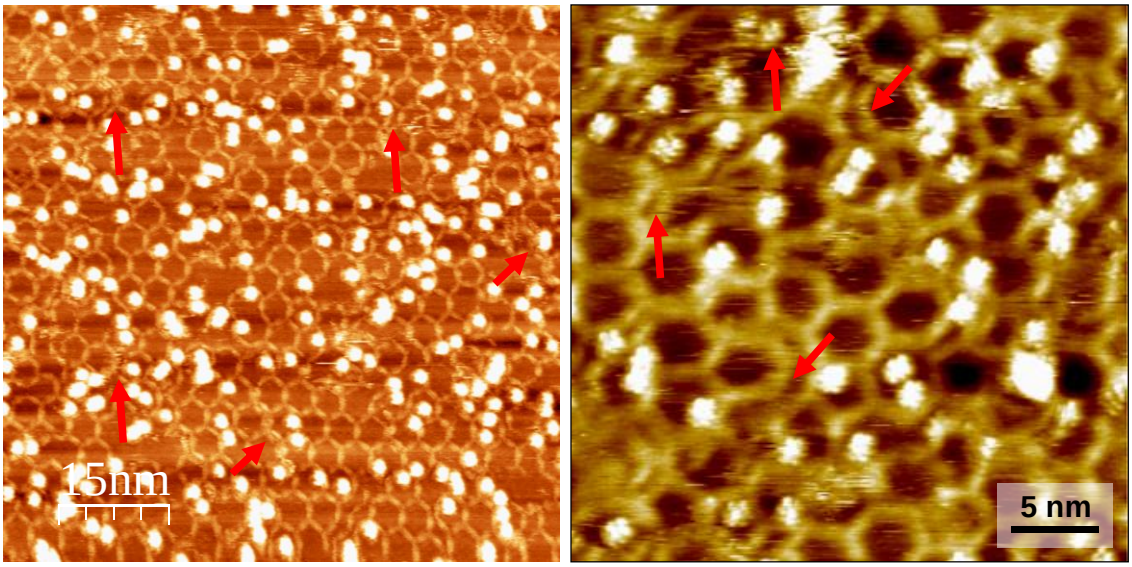

Figure S3d. High-resolution STM images of $sCOF_{BTA\text{-}DATP}$ on a high-density modified HOPG surface (60000–90000 grafted TBD species/μm^2). Imaging conditions: I_{set} = 50 pA, V_{bias} = -0.66 V.

Above a density of grafting of about 60 000 molecules/µm^2, the number of domains increases and so does their dispersion. The sCOF sheet size dispersion becomes broader as the density of grafting increases. Since the TBD molecules are grafted randomly on the HOPG surface,[3] agglomeration of pins or some empty areas can be encountered. This situation influences the sCOF flake size and their general dispersion (Fig. S3e).

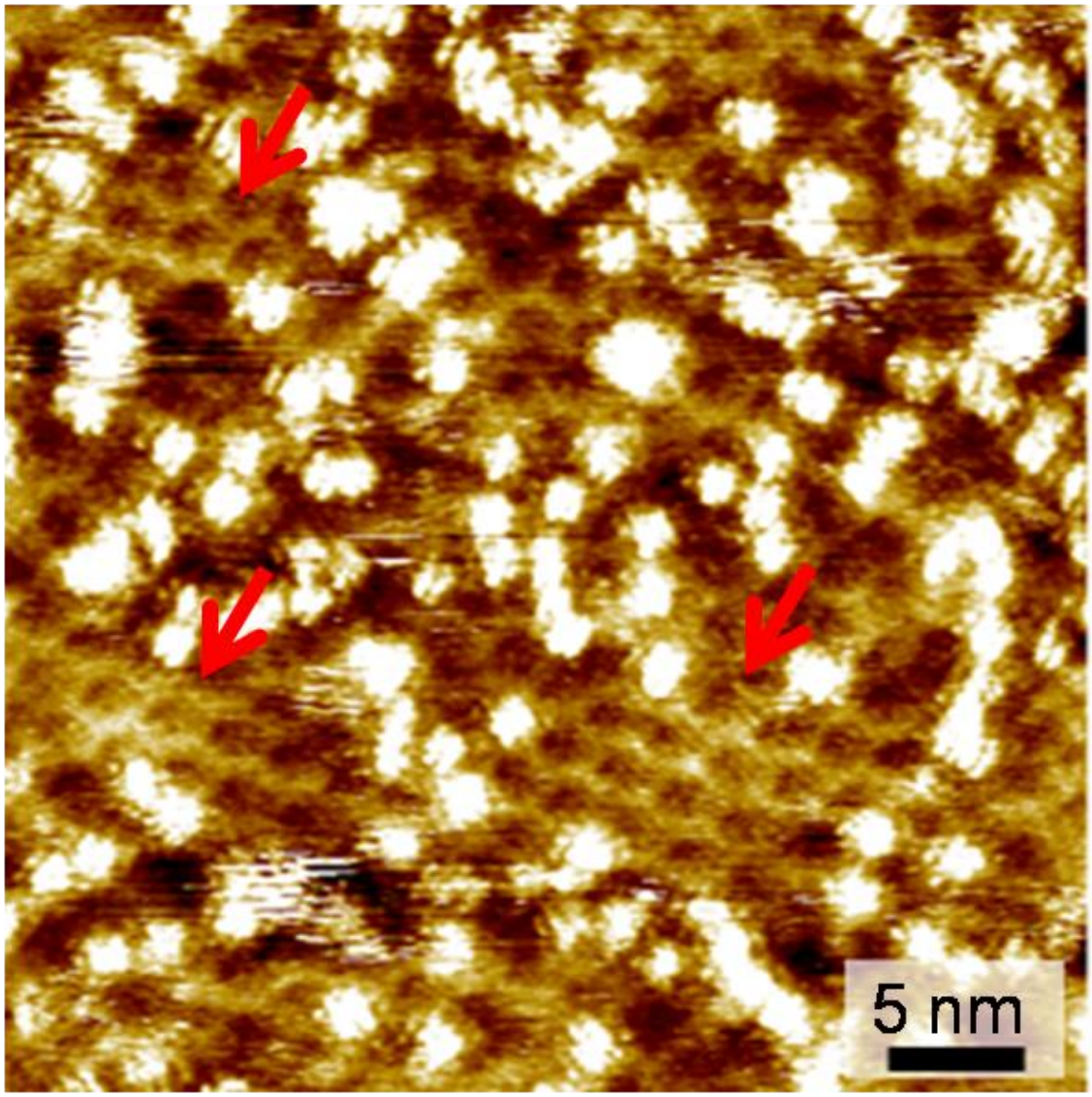

Figure S3e. STM image of $sCOF_{BTA\text{-}PDA}$ on a modified HOPG surface with high density of grafted TBD species. The red arrows indicate some large sCOF flakes due to the local absence of grafted molecules.

In very high-resolution STM images, TBD grafted molecules have an unequivocal appearance. They are easily discerned from occasional white spots that are inherent to the Schiff-base on-surface reaction and correspond to unreacted monomers or polymeric aggregates.

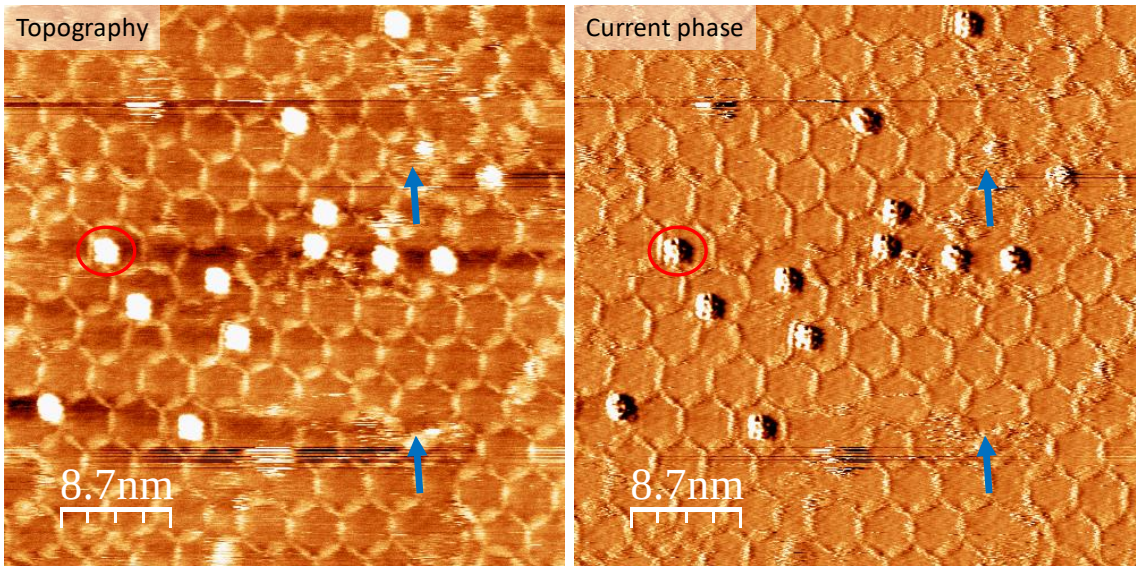

Figure S3f. STM topography image of $sCOF_{BTA\text{-}DATP}$ on a modified HOPG surface with low density of grafted TBD species (left). Corresponding STM current phase image (right). While grafted molecules (circled in red) can be seen as bulky clusters displaying four lobes and a shadow, typical "white spots" (blue arrows) corresponding to unreacted monomers or agglomerates are seen as lower and fuzzier features.

S4. Nanoshaving experiments.

The nanolithography experiments were realized by scanning a small surface area with high current and low bias (typically 0.2 nA and -0.001 V). Under these conditions, the grafted aryl species were locally removed. It was then assessed how the sCOF system responded to the removal of the covalently attached bulky molecules. The nanoshaved area was scanned for several minutes afterwards. While the network is affected, the sCOF remains adsorbed on the surface. The observed changes could be due to the harsh nanoshaving conditions, which could add instability to the system. Another possibility is that the elimination of grafted molecules results in a vacancy on the surface, which in turn triggers bond breaking and reforming in this on-surface dynamic covalent chemistry Schiff-base reaction.

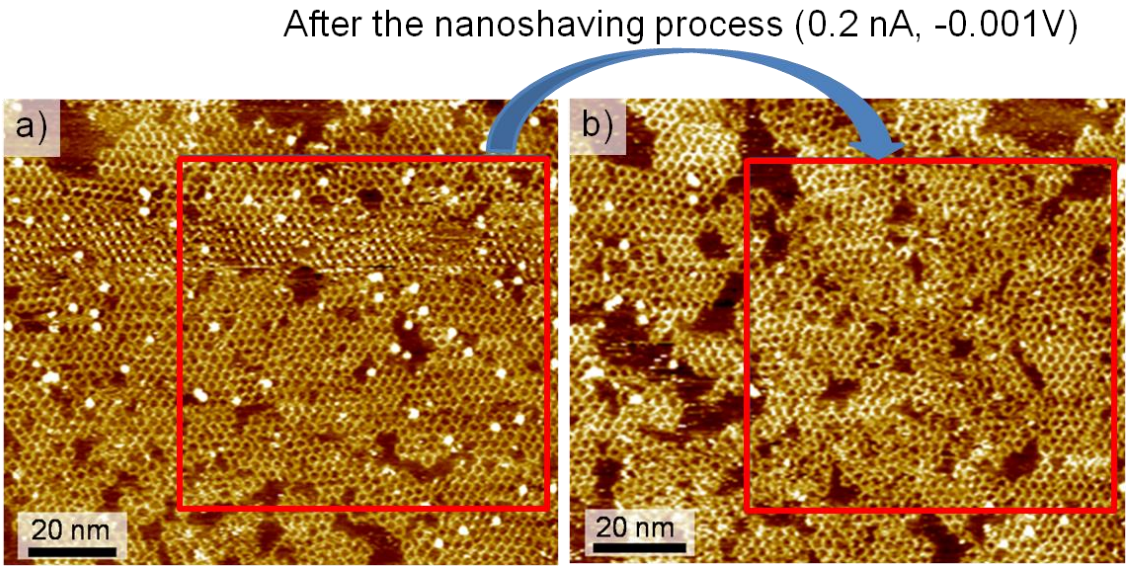

Figure S4a. Consecutive images (3 min time lapse) after the nanoshaving process of $sCOF_{BTA\text{-}PDA}$ on HOPG surface with low density of the grafted species. Imaging conditions: I_{set} = 110 pA, V_{bias} = -0.2 V.

As the density of grafting increases, the underlying sCOF is more affected by the nanoshaving process. The 2D polymer is destroyed but starts regrowing in the newly created corral taking into consideration the orientation of the surrounding 2D sCOF flakes. The on-surface reaction proceeds from the dangling ends on the edges of the nanoshaved area and thus follows the same direction than the previous polymer.

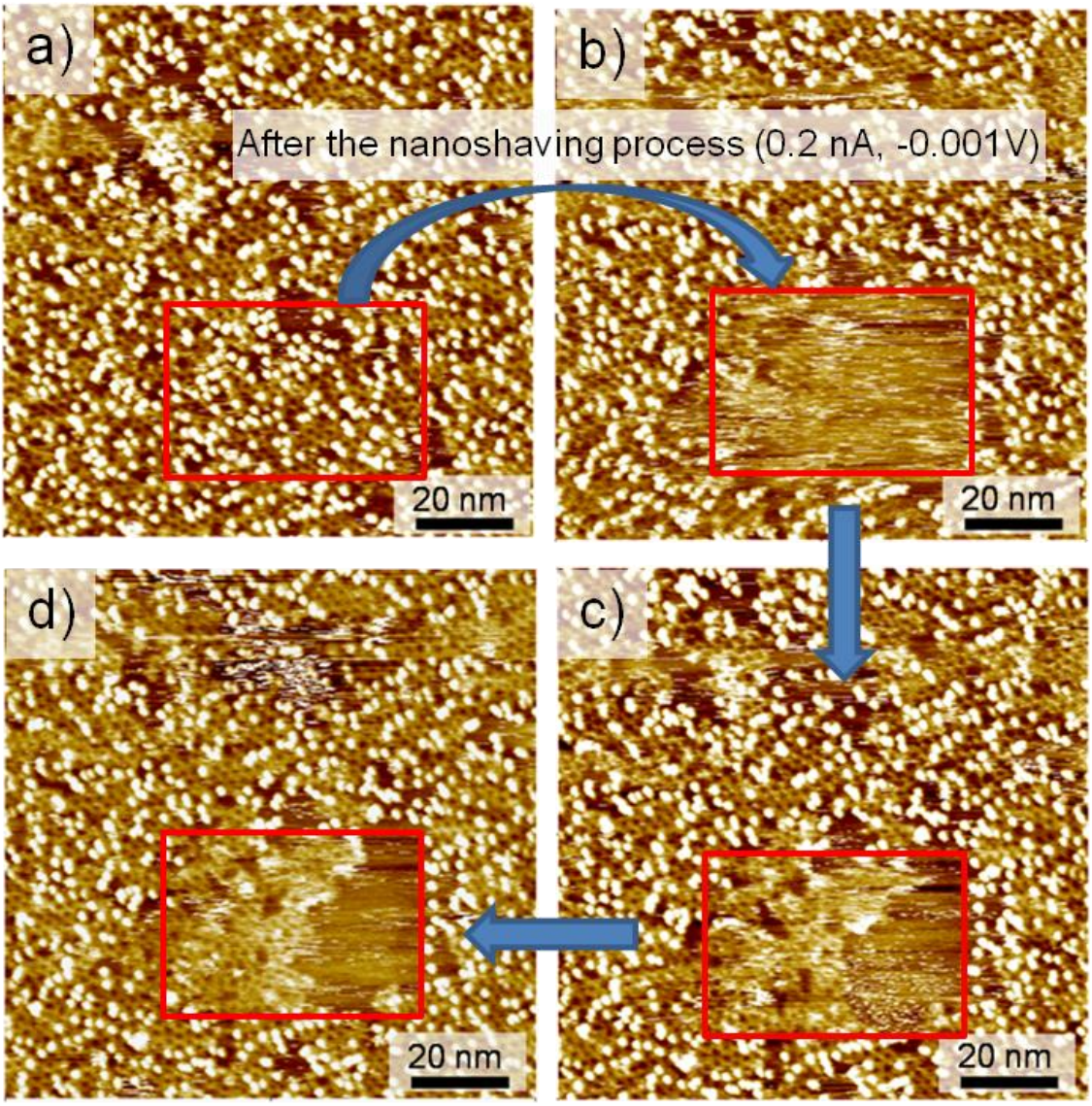

Figure S4b. Consecutive images (5 min time lapse between b) and d)) after the nanoshaving process of $sCOF_{BTA\text{-}PDA}$ on modified HOPG with very high density of grafted species and regeneration of the sCOF. Imaging conditions: I_{set} = 60 pA, V_{bias} = -0.6 V.

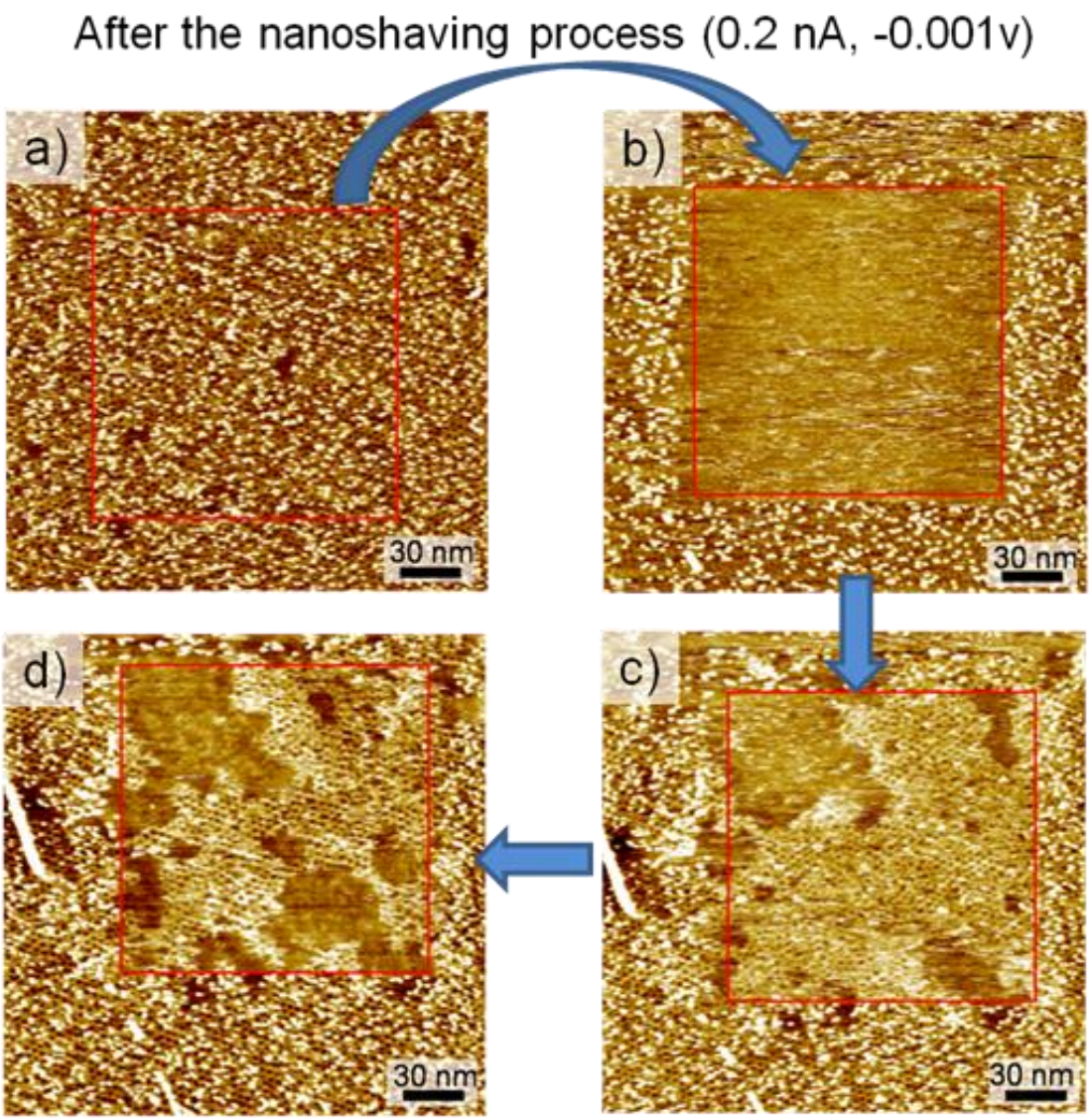

Figure S4c. Consecutive images (9 min time lapse between b) and d)) of the nanoshaving process of $sCOF_{BTA\text{-}DATP}$ on modified HOPG with high density of grafted species and regeneration of the sCOF. Imaging conditions: I_{set} = 60 pA, V_{bias} = -0.76 V.

S5. Towards 2D polymer engineering.

By modifying graphitic surfaces in a controlled manner, and by specifically removing the grafted aryl molecules in a second step, one can prepare sCOFs of pre-determined dimensions by taking advantage of the dynamic nature of the system that is able to regenerate at room temperature and under ambient conditions.

As a proof-of-concept experiment, we prepared a high density grafted HOPG substrate (0.4 mM TBD) and drop-casted the appropriate precursors for the formation of $sCOF_{BTA\text{-}AABA}$. Under these conditions, the corresponding sCOF cannot form properly (see Fig. 2f of the manuscript). Small linear oligomers, disordered molecules and small 2D sCOF oligomers can be observed on the grafted sample (Fig. S5a). After nanoshaving under controlled conditions (0.2 nA; -0.01 V; 8 µm/s, and a vertical distance of 0.9 nm between consecutive shaving lines), both grafted TBD molecules and the imine-based products were removed from the surface. As from the next scan, hexagonal and porous $sCOF_{BTA\text{-}AABA}$ starts to be visible. Although $sCOF_{BTA\text{-}AABA}$ could not cover the totality of the nanoshaved area (a small polymer-free area can be seen in the top left corner of the nanoshaved corral) and remains interconnected to other imine-based fragments adsorbed on the remaining grafted surface, a 2D polymer of pre-determined size and shape could be prepared. This sCOF oligomer is free of grafted molecules, which affect the 2D polymer growth. Therefore, the $sCOF_{BTA\text{-}AABA}$ flake formed has larger molecular weight than the other products that can be found on the surface. In this way, this approach has proven to be able to control size, shape and affect the polydispersity of the final product of this 2D polymerization.

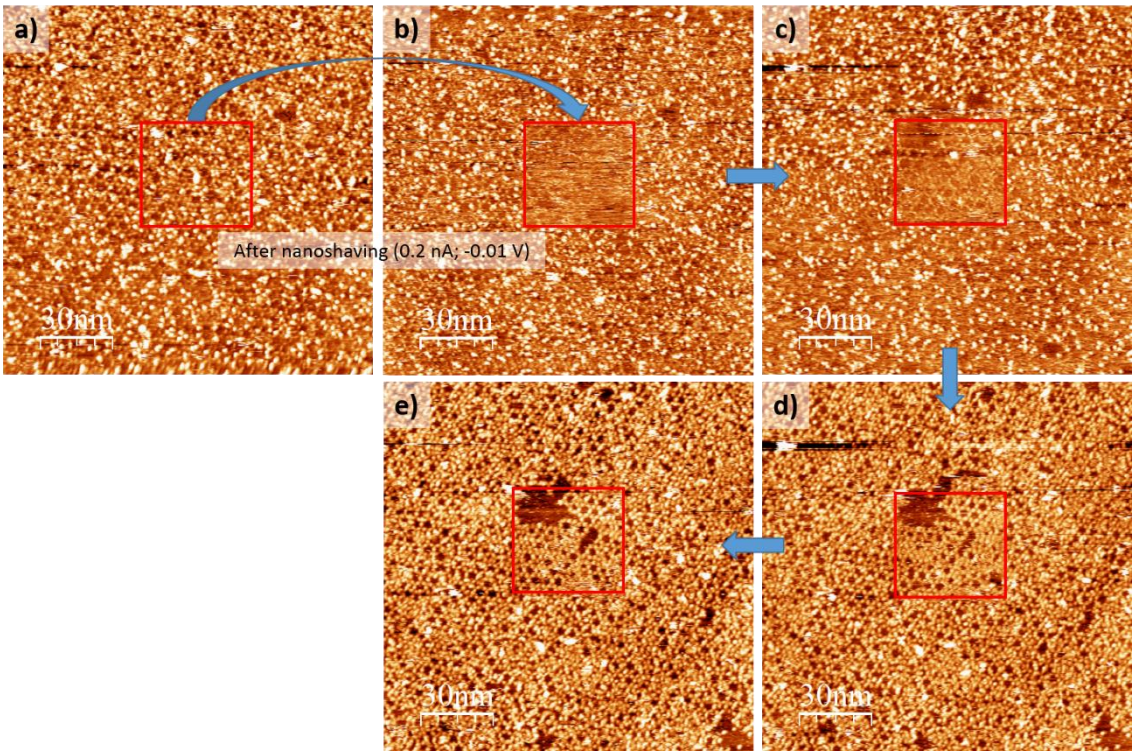

Figure S5. Consecutive images (14 min time lapse between b) and d)) after the nanoshaving process of $sCOF_{BTA\text{-}AABA}$ on modified HOPG with high density of grafted species and subsequent formation of a BTA and AABA based sCOF oligomer of 42 (height) x 44.5 (width) nm^2. Imaging conditions: I_{set} = 60 pA, V_{bias} = -0.80 V.

S6. Characterization data of the compound AABA.

^{1}H NMR spectrum

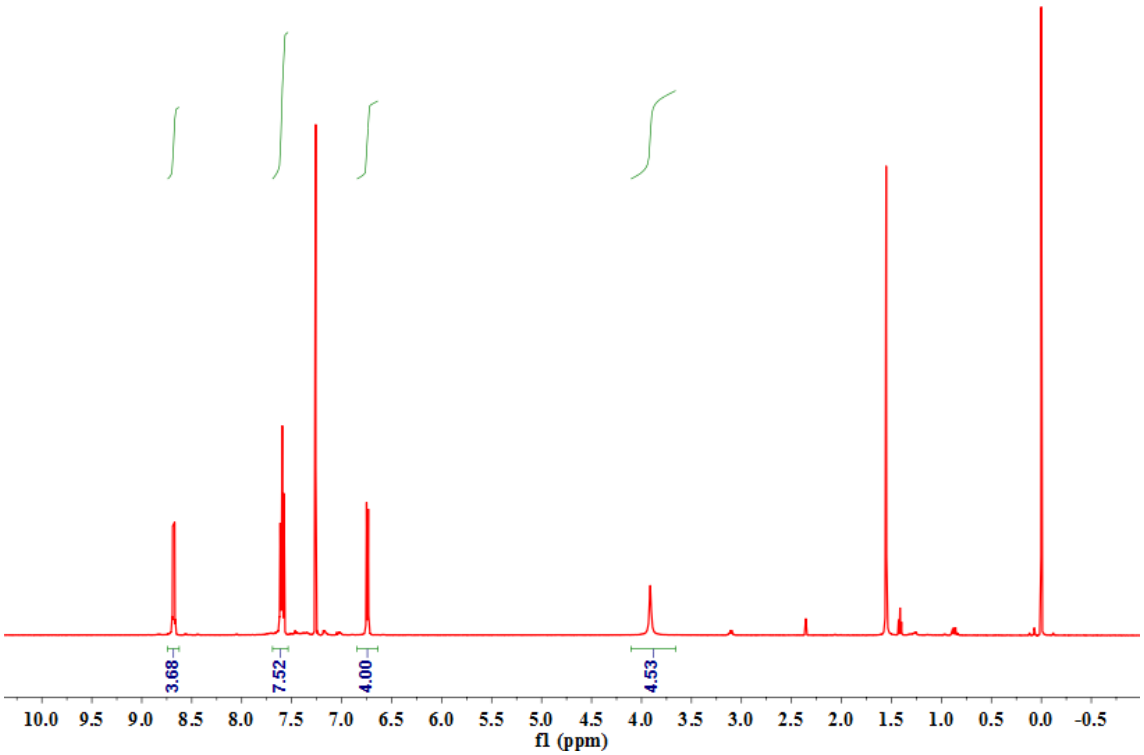

^{1}H NMR (500 MHz, $CDCl_3$): δ 8.70 – 8.67 (m, 4H), 7.62 – 7.57 (m, 8H), 6.74 (d, J = 8.5 Hz, 4H), 3.91 (s, 4H).

Mass Spectrometry spectrum

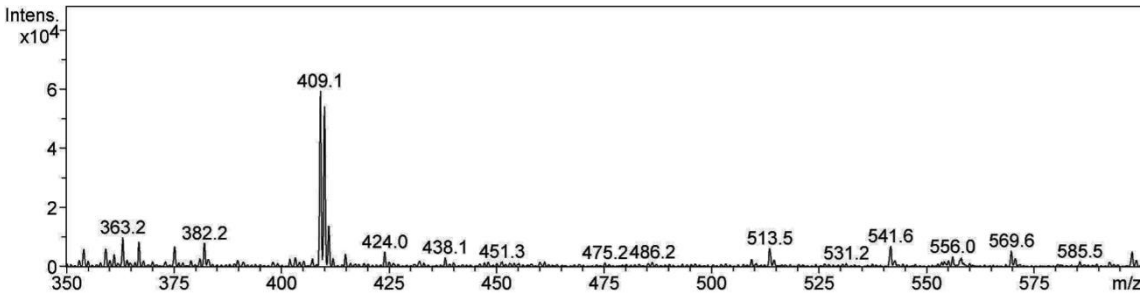

MS (ESI): m/z 409.1 [M^+]

1. I. Horcas, R. Fernández, J. M. Gómez-Rodríguez, J. Colchero, J. Gómez-Herrero and A. M. Baro, *Review of Scientific Instruments*, 2007, **78**, 013705.
2. J. Greenwood, T. H. Phan, Y. Fujita, Z. Li, O. Ivasenko, W. Vanderlinden, H. Van Gorp, W. Frederickx, G. Lu, K. Tahara, Y. Tobe, H. Uji-i, S. F. L. Mertens and S. De Feyter, *ACS Nano*, 2015, **9**, 5520-5535.
3. A. M. Braganca, J. Greenwood, O. Ivasenko, T. H. Phan, K. Mullen and S. De Feyter, *Chem. Sci.*, 2016, **7**, 7028-7033.
4. Y. Yu, J. Lin, Y. Wang, Q. Zeng and S. Lei, *Chem. Commun.*, 2016, **52**, 6609-6612.
5. M. Imoto, M. Takeda, A. Tamaki, H. Taniguchi and K. Mizuno, *Research on Chemical Intermediates*, 2009, **35**, 957.
6. L. Xu, X. Zhou, W. Q. Tian, T. Gao, Y. F. Zhang, S. Lei and Z. F. Liu, *Angew. Chem. Int. Ed.*, 2014, **53**, 9564-9568.
7. L. Xu, X. Zhou, Y. Yu, W. Q. Tian, J. Ma and S. Lei, *ACS Nano*, 2013, **7**, 8066-8073.
8. J.-Y. Yue, X.-H. Liu, B. Sun and D. Wang, *Chem. Commun.*, 2015, **51**, 14318-14321.
9. J. Sun, X. Zhou and S. Lei, *Chem. Commun.*, 2016, **52**, 8691-8694.
10. L. Xu, L. Cao, Z. Guo, Z. Zha and S. Lei, *Chem. Commun.*, 2015, **51**, 8664-8667.